UAV-Assisted Cellular Communication: Joint Trajectory and Coverage Optimization

Yang Li, Heli Zhang, Hong Ji, and Xi Li
Key Laboratory of Universal Wireless Communications, Ministry of Education
Beijing University of Posts and Telecommunications
Beijing, P.R. China
Email: {liyang, zhangheli, jihong, lixi}@bupt.edu.cn

2021 IEEE Wireless Communications and Networking Conference (WCNC) | 978-1-7281-9505-6/20/$31.00 ©2021 IEEE | DOI: 10.1109/WCNC49053.2021.9417264

***Abstract*—Unmanned aerial vehicle (UAV)-assisted cellular communication is regarded as a promising solution for the data traffic offloading of cell-edge users, who often have throughput bottlenecks. As an air base station (ABS), UAV has high mobility, flexible deployment, high probability of line-of-sight (LoS) link, etc. In this paper, we propose a cooperation schema between multiple ground base stations (GBSs) and UAV to optimize the coverage of GBSs and UAV. Firstly, we jointly optimize the coverage division, the spectrum allocation, and UAV's trajectory to maximize the minimum throughput of cell-edge users. Secondly, we propose an iterative algorithm to solve the non-convex problem and obtain a suboptimal solution. Finally, in the simulation, the other two strategies are compared with the algorithm proposed in this paper to prove its effectiveness.**

***Index Terms*—UAV, ABS, coverage division, spectrum allocation, trajectory optimization, cellular offloading.**

I. Introduction

In the future, the fifth generation (5G) mobile communication networks will provide seamless, ubiquitous connection services, and support at least 1000 times the traffic and 100 billion connected wireless devices [1]. The popularity of the Internet of Things will greatly increase 5G and Beyond 5G wireless network data traffic. However, traditional cellular networks have many problems when faced with a surge in data traffic. Firstly, ground base stations (GBSs) in traditional cellular networks are usually deployed statically, which makes it difficult to deal with the traffic offloading of edge users in communication hotspots. Secondly, the cell edge users in the hotspot are far away from the GBS, and their channel status is poor [2]. Finally, facing a sudden increase in traffic, it is difficult for GBS to flexibly adapt to this change [3]. As air base station (ABS), unmanned aerial vehicles (UAV) can greatly improve the capacity, coverage, and energy efficiency of cellular networks due to their mobility and flexibility [4]. Therefore, extensive research is increasingly focusing on heterogeneous cellular networks assisted by UAV [5].

Recent years, critical challenges for UAV-assisted cellular networks, such as optimal deployment, trajectory optimization, and energy efficiency, have achieved representative results, such as [6] - [13]. In a multiuser scenario, paper [6] proposed a new heterogeneous network in which multiple UAVs are deployed on the edge of a single cell. The authors in [7] considered energy-efficient UAV-assisted networks, where the UAV returns to the charging position before the energy is exhausted. Papers [8] - [9] studied how to maximize the minimum throughput of users, so that each user can obtain better throughput. The authors in [10] jointly optimized user division, resource allocation, and UAV's path planning to improve the energy efficiency of UAV. In [11], the authors considered a scenario where a user can only connect to GBS or UAV at the same time, and optimized the flight path of the UAV. In the paper [12], the author maximized the minimum throughput of users by optimized communication design and the UAV's path planning. As indicated in [13], the author modeled the UAV-assisted cellular networks as the Poisson point process in a two-dimensional space. The UAV is located in the center of this area and continues to provide services to users. However, previous studies leave the coverage division between multiple GBSs and UAV out of consideration, which makes it difficult for UAV to effectively assist each GBS [14].

In this paper, we propose new hybrid cellular networks which take into account the cooperation between multiple GBSs and UAV, and dynamically divide the coverage area. The spectrum allocation, coverage division, and the trajectory of UAV are jointly optimized to improve the quality of service (QoS) of cell-edge users. For this complex problem, we propose a sub-optimal algorithm based on successive convex optimization technology. The simulation results show that the algorithm proposed in this paper can effectively improve the throughput of cell-edge users.

II. System Model and Problem Formulation

A. System Model

As shown in Fig.1, we consider three cells with radius of r_{CELL}, where the GBS with coverage radius of $r_{GBS_j}, j \in \{1,2,3\}$ is located in the center of the cell. A UAV is deployed to offload data traffic for the cell-edge users. In this paper, downlink communications from GBS/UAV to users is considered. The user's locations in the three cells follow randomly and uniformly distribution with density $\lambda_{GBS_j}, j \in \{1,2,3\}$. We denote the horizontal coordinate of the i-th user as $w_i = \{x_i, y_i\} \in R^{2\times 1}$.

The UAV makes T periodic flights around the edges of three adjacent cells to provide services to edge users, with start point and end point at the same location. The UAV flies at a

978-1-7281-9505-6/21/$31.00 ©2021 IEEE

Authorized licensed use limited to: Beijing Information Science & Tech Univ. Downloaded on March 19,2023 at 02:47:48 UTC from IEEE Xplore. Restrictions apply.

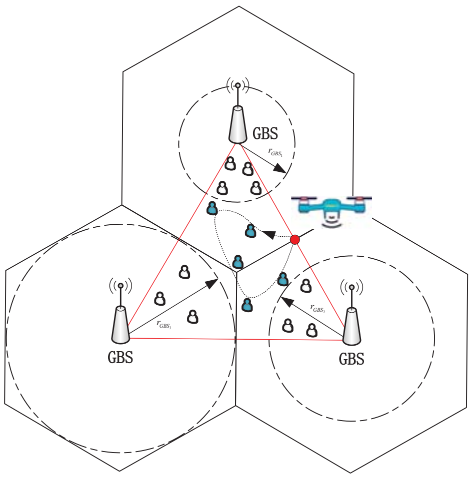

Fig. 1. System model.

fixed altitude H_{UAV} with maximum speed $V_{\max}$. We denote the half-beam width of the UAV antenna as θ, then there is $\tan\theta = \frac{r_{UAV}}{H_{UAV}}$, and r_{UAV} is the radius of the ground area that the UAV can cover at a certain location. We assume that the UAV has an ideal wireless backhaul link to GBS and that the link operates on a separate band.

The total time length T is divided into N equal time slots. We must choose the value of N reasonably so that the position of the UAV in each time slot is almost unchanged. As such, the UAV's position $q[n]$ in a specific time slot $n, n \in \{1,2,3\cdots N\}$ can be represented by a coordinate point on a two-dimensional plane [**?**], that is, $q[n] = \{x[n], y[n]\}, n \in \{1,2,3\cdots N\}$. Therefore, the flight trajectory of the UAV should meet the following conditions: $q[1] = q[N], \|q[n+1] - q[n]\|^2 \le (V_{\max}\frac{T}{N})^2$.

It is assumed that the distance between the three GBSs is relatively long, so there is no interference between them. The whole bandwidth is assumed to be B. In order to avoid interference between the UAV and GBSs, the available bandwidth of UAV is $\rho B, 0 < \rho < 1$, and the bandwidth that each GBS can allocated is $(1-\rho)B, 0 < \rho < 1$. In each slot, the UAV serves users in the range of r_{UAV} through orthogonal frequency division multiple access (OFDMA), and equal bandwidth is allocated to each user. Similarly, the GBSs also serve users in $r_{GBS_j}, j \in \{1,2,3\}$ in the same way.

As described in [6], the channel power gain from the j-th GBS to the i-th user is

$$h_{GBS_j i} = \frac{\beta_0 V_i}{({H_{GBS}}^2 + {r_{GBS_j i}}^2)^{\frac{\alpha}{2}}}, \tag{1}$$

where $V_i \sim EXP(1)$ denotes the exponential distribution, β_0 represents the channel gain of $d = 1m$, and α is the path loss exponent. $r_{GBS_j i}$ denotes the horizontal distance between the i-th user and the j-th GBS, and H_{GBS} represents the height of GBS. We adopt the same manipulations in [6], where the average signal-to-noise ratio (SNR) among users is defined as γ_{GBS_j}. Then, we have

$$\gamma_{GBS_j} = \frac{P_{GBS} G_{GBS} \beta_0}{\sigma^2 B_{GBS_j} (H_{GBS}^2 + r_{GBS_j}^2)^{\alpha/2}}, \tag{2}$$

where σ^2 denotes the power spectrum density of additive white Gaussian noise and G_{GBS} denotes the GBS's omnidirectional antenna gain, P_{GBS} is the transmit power of GBS, and $B_{GBS_j} = \frac{6(1-\rho)B}{\pi r_{GBS_j}^2 \lambda_{GBS_j}}$ is the bandwidth allocated to each user.

We assume that the channel between the UAV and the user follows the free space loss model [8]. Therefore, the channel power gain from UAV to the l-th user is expressed as

$$h_{UAVl}^{[n]} = \frac{d_0}{{H_{UAV}}^2 + \|q[n] - w_l\|^2}, \tag{3}$$

where d_0 denotes the channel power gain, and $\|q[n] - w_l\|$ represents the horizontal distance between l-th user and UAV.

B. Problem Formulation

Derived from the previous section, the minimum instantaneous achievable throughput of users associated with GBSs can be given as

$$R_{GBS_j} = B_{GBS_j} \log_2(1 + \gamma_{GBS_j} V_i). \tag{4}$$

Due to the small-scale fading between GBS and users, an outage event will occur when R_{GBS_j} is less than the given throughput threshold R_{GBSth}. The outage probability of the worst link between GBS and users can given by

$$\begin{aligned} P_{out,GBS_j} &= P_r\left(B_{GBS_j}\log_2(1+\gamma_{GBS_j}V) < R_{GBSth}\right) \\ &= P_r\left(V < \left(2^{R_{GBSth}/B_{GBS_j}} - 1\right)/\gamma_{GBS_j}\right) \\ &= 1 - \exp\left(-\left(2^{R_{GBSth}/B_{GBS_j}} - 1\right)/\gamma_{GBS_j}\right), \end{aligned} \tag{5}$$

which is an increasing function of R_{GBSth}. It can be proved by a derivation that R_{GBS_j} is a decreasing function of r_{GBS_j} and ρ, and thus P_{out,GBS_j} is an increasing function of r_{GBS_j} and ρ.

The throughput that the l-th cell edge user can obtain in the time slot n is

$$R_{UAVl}^{[n]} = \frac{\rho B}{L_n} \log_2(1 + \frac{P_{UAV} h_{UAVl}^{[n]}}{\rho B \sigma^2}), \tag{6}$$

where L_n is the number of users served by the UAV in the n-th time slot, and P_{UAV} represents the maximum transmission power of the UAV. Thus, the average throughput of l-th user within T is

$$R_{UAVl} = \frac{1}{T} \sum_{n=1}^{N} R_{UAVl}^{[n]}. \tag{7}$$

We jointly optimize the spectrum allocation, the coverage division, and UAV's trajectory to maximize the minimum

Authorized licensed use limited to: Beijing Information Science & Tech Univ. Downloaded on March 19,2023 at 02:47:48 UTC from IEEE Xplore. Restrictions apply.

average throughput of cell-edge users, and keep the throughput of other users greater than or equal to R_{GBSth} and define $R_{UAVth} = \min_{l \in L} R_{UAVl}$. Mathematically, the research problem can be expressed as:

$$\begin{aligned} &\max_{\{r_{GBS_j}, \rho, q[n]\}} R_{UAVth} \\ \text{s.t.}\quad & C1: P_{out,GBS_j} \le P_{th}, \\ & C2: R_{UAVth} \le R_{UAVl}, \forall l \in L, \\ & C3: 0 \le \rho \le 1, \\ & C4: \|q[n+1] - q[n]\|^2 \le (V_{\max}\frac{T}{N})^2, \\ & C5: q[1] = q[n], \\ & C6: 0 \le r_{GBS1}, r_{GBS2}, r_{GBS3} \le r_{CELL}, \end{aligned} \tag{8}$$

where $C3$ is a constraint on the spectrum allocation between the UAV and the GBSs, $C4$ and $C5$ are related to the UAV trajectory, and $C6$ is a constraint on the coverage radius of the three GBSs. The constraint C2 is non-convex with respect to UAV trajectory variables $q[n]$. Therefore, problem (8) is a complex non-convex optimization problem. In the next chapter, we propose an iterative algorithm to obtain the suboptimal solution.

III. Proposed Algorithm

The problem (8) is a non-convex complex problem that is difficult to solve with standard convex optimization techniques. In this section, we propose an overall iterative algorithm based on successive convex optimization technique.

A. GBSs Coverage Optimization

Given UAV trajectory and bandwidth allocation ρ, the optimization problem (8) can be simplified as:

$$\begin{aligned} &\max_{\{r_{BS_j}\}} R_{UAVth} \\ \text{s.t.}\quad & C1: P_{out,GBS_j} \le P_{th}, \\ & C2: R_{UAVth} \le R_{UAVl}, \forall l \in L, \\ & C3: 0 \le r_{GBS1}, r_{GBS2}, r_{GBS3} \le r_{CELL}. \end{aligned} \tag{9}$$

Observing the objective function and constraints, it can be found that the objective function increases monotonically with respect to r_{GBS_j}, and C1 also increases monotonically with respect to r_{GBS_j}. Thus, the solution of r_{GBS_j} can be obtained by bisection search when both ρ and UAV trajectory are given.

Jointly optimizing spectrum allocation and trajectory is still a complex non-convex problem. Further, we decompose it into two sub-problems and then obtain suboptimal solutions.

B. Spectrum Allocation Optimization

For a fixed UAV trajectory and coverage division, the optimization problem (8) can be simplified as follows:

$$\begin{aligned} &\max_{\{\rho\}} R_{UAV\mathrm{th}} \\ \text{s.t.}\quad & C1: P_{out,GBS_j} \le P_{th}, \\ & C2: R_{UAVth} \le R_{UAVl}, \forall l \in L, \\ & C3: 0 \le \rho \le 1. \end{aligned} \tag{10}$$

It can be verified that R_{UAVth} and P_{out,GBS_j} are both increasing function of ρ. Therefore, ρ should be set to the maximum value that satisfies condition $P_{out,GBS_j} \le P_{th}$, so as to maximize R_{UAVth}. Perform a binary search on ρ in the range of 0 to 1, and the maximum value that satisfies the constraint is the optimal solution of ρ.

C. UAV Trajectory Optimization

For a given bandwidth allocation ρ and coverage division, the problem can be simplified as:

$$\begin{aligned} &\max_{\{q[n]\}} R_{UAVth} \\ \text{s.t.}\quad & C1: R_{UAVth} \le R_{UAVl}, \forall l \in L, \\ & C2: \|q[n+1] - q[n]\|^2 \le (V_{\max}\frac{T}{N})^2, \\ & C3: q[1] = q[n]. \end{aligned} \tag{11}$$

Obviously, R_{UAVth} is non-concave concerning trajectory $q[n]$, but convex with respect to $\|q[n] - w_l\|^2$. We can find the lower bound of any point through its first-order Taylor expansion. In each iteration step, the C1 expression will be replaced with its lower bound [14]. Define $q^r[n], \forall n \in \{1, 2, 3 \cdots N\}$ as the trajectory of UAV given at r-th iteration.

$$\begin{aligned} R_{UAVl}^{[n]} &= \frac{\rho B}{L_n}\log_2(1 + \frac{P_{UAV} d_0}{\rho B \sigma^2 ({H_{UAV}}^2 + \|q_0[n] - w_l\|^2)}) \\ &> \frac{\rho B}{L_n}\log_2(1 + \frac{\frac{P_{UAV} d_0}{\rho B \sigma^2}}{{H_{UAV}}^2 + \|q_0[n] - w_l\|^2}) - A_l^{[n]} \\ &= R_{lbUAVl}^{[n]}, \end{aligned} \tag{12}$$

where

$$A_l^{[n]} = \frac{P_{UAV} d_0 (\|q[n] - w_l\|^2 - \|q_0[n] - w_l\|^2)}{L_n \ln 2 ({H_{UAV}}^2 + \|q_0[n] - w_l\|^2) B_l^{[n]}}, \tag{13}$$

$$B_l^{[n]} = {H_{UAV}}^2 + \|q_0[n] - w_l\|^2 + \frac{P_{UAV} d_0}{\rho B \sigma^2}. \tag{14}$$

We remove the remainder of the first-order Taylor expansion and use it as the lower bound of the original objective function. Obviously, the lower bound is concave about $q[n], \forall n \in \{1, 2, 3 \cdots N\}$. Replace $R_{UAVl}^{[n]}$ with $R_{lbUAVl}^{[n]}$ to get the new objective function and constraints as follows:

Authorized licensed use limited to: Beijing Information Science & Tech Univ. Downloaded on March 19,2023 at 02:47:48 UTC from IEEE Xplore. Restrictions apply.

$$\begin{aligned}&\max_{\{q[n]\}} \min_{L} \frac{1}{T}\sum_{n=1}^{N} R_{lbUAVl}^{[n]} \\ \text{s.t.}\quad & C1: R_{UAVth} \le \frac{1}{T}\sum_{n=1}^{N} R_{lbUAVl}^{[n]}, \forall l \in L, \\ & C2: \left\|q\left[n+1\right]-q\left[n\right]\right\|^2 \le \left(V_{\max}\frac{T}{N}\right)^2, \\ & C3: q\left[1\right]=q\left[n\right],\end{aligned} \tag{15}$$

where $C1$ is concave with respect to $q\left[n\right], \forall n \in \{1,2,3\cdots N\}$, $C2$ is a quadratic constraint, and $C3$ is a linear constraint. So, the problem (15) is a quadratic programming problem with quadratic constraints. Similarly, we can solve this problem by the standard convex optimization. It is noteworthy that the new problem (15) can only replace the original problem (11) approximately, and its optimal result is the lower bound of (11).

D. Overall Optimization Algorithm and Convergence Analysis

Derived from the previous section, we decompose the problem into three parts and propose an overall iterative algorithm based on the gradient descent method. During each iteration, the $r_{GBS_j}, j \in \{1,2,3\}$, spectrum allocation and trajectory are optimized by solving problems (9),(10) and (15) respectively. When optimizing one of the parameters, the value of the other parameters is fixed. The initial value of the next iteration uses the result of the previous iteration. The entire algorithm is illustrated as Algorithm 1.

Next, the proof of convergence of Algorithm 1 is introduced. At the r-th iteration in step 5, with given $q^r[n]$ and ρ^r, the optimal solution of problem (9) is denoted as $r_{GBS_j}^{r+1}$, we can get the inequality as follows

$$\begin{aligned}&R_{UAVth}\{r_{GBS_j}^{r+1}, \rho^{r+1}, q^{r+1}[n]\} \\ &\ge R_{UAVth}\{r_{GBS_j}^{r+1}, \rho^{r+1}, q^{r}[n]\} \\ &\ge R_{UAVth}\{r_{GBS_j}^{r+1}, \rho^{r}, q^{r}[n]\} \\ &\ge R_{UAVth}\{r_{GBS_j}^{r}, \rho^{r}, q^{r}[n]\},\end{aligned} \tag{16}$$

which can prove that Algorithm 1 will not decrease in each iteration. And the problem (9) has a certain upper bound value. Therefore, it is guaranteed that Algorithm 1 is convergent.

E. UAV Trajectory Initialize

The initialization of the trajectory will affect the results of the algorithm. In this section, we design a less complex initial value setting method for UAV trajectory. First, the UAV's flight speed is $V, 0 < V < V_{\max}$, and the center of the circular trajectory is the center point of entire area. Suppose the radius is $r_{traInit}$, and for a given T, there is $2\pi r_{traInit} = VT$. From the analysis above, we design the initial trajectory of the UAV as a circular trajectory with the center being $\{0, 150\}$ and the radius being $2\pi r_{traInit} = VT$, and the speed of the UAV remains at $V, 0 < V < V_{\max}$.

Therefore, as long as the values of $r_{traInit}$ and $V, 0 < V < V_{\max}$ are determined, the initialization trajectory of the UAV is obtained. The path where the UAV covers the largest number of users is the best trajectory. Assuming $r_{traInit}$ is an integer, there is $0 < r_{traInit} < \frac{V_{\max}T}{2\pi}, r_{traInit} \in R$. Search each value of $r_{traInit}$ to get the amount of users that the UAV covers under the trajectory. We take $r_{traInit}$ as the value when the UAV covers the biggest amount users. If the number of users served by UAV is the same under two different $r_{traInit}$, the smaller is taken. By defining $\theta_n = 2\pi\frac{n}{N}$, then we can get $q_0[n] = \{r_{traInit}\cos\theta_n, 150 + r_{traInit}\sin\theta_n\}$.

Algorithm 1 Joint coverage division, spectrum allocation, and trajectory optimization

1: Input: R_{GBSth}, N_{BS_j}, T, N, H_{UAV}, H_{BS}, θ, $V_{\max}$, B, P_{GBS}, P_{UAV}, β_0, d_0, σ^2, α, r_{CELL}.
2: Output: suboptimal solution of the problem (9). The coverage range of the GBSs r_{GBS_j}, the spectrum allocation ρ, and UAV's trajectory $q[n]$.
3: Let r = 0, r_{GBS_j} = 0
4: Initialize $q^0[n]$, ρ^0
5: **repeat**
6: Solve problem (10) with $q^r[n]$ and ρ^r, and save the result as $r_{GBS_j}^{r+1}$
7: Solve problem (11) with $q^r[n]$ and $r_{GBS_j}^{r+1}$, and save the result as ρ^{r+1}
8: Solve problem (16) with ρ^{r+1} and $r_{GBS_j}^{r+1}$, and save the result as $q^{r+1}[n]$
9: Update $r = r + 1$
10: **until** $R_{UAVth}^{r+1} - R_{UAVth}^{r} < \varepsilon$

IV. Simulation Results

In this section, we verify the effectiveness of the algorithm proposed in this paper by comparing with the other two algorithms. We consider an area consisting of three cells. In the simulation, we assume that $r_{CELL} = 300m$, $H_{UAV} = 100m$, $H_{GBS} = 50m$, $\theta = 30°$, $V_{\max} = 35m/s$, $B = 1MHZ$, $P_{GBS} = 46dBm$, $P_{UAV} = 20dBm$, $G_{GBS} = 16dBi$ $\beta_0 = -60dB$, $d_0 = -30dB$, $\sigma^2 = -160dBm$, $\alpha = 3$, $R_{GBSth} = 1.5Mbps$.

To prove the effectiveness of proposed algorithm in this paper, we compare it with two schemes. The first scheme (NDCD) dosn't take into account the dynamic coverage division and the r_{GBS_j} is fixed as half of the r_{CELL}. This scheme assume that the UAV trajectory is circular [10] and only one user served by UAV in a slot. In the second scheme (NUAV), all the users is served by GBSs without UAV assistance. We suppose that the total number of users in the three cells increases from 10 to 80. Considering the uneven distribution of users in the three cells, we set the number of users in the three cells as $\lambda_{GBS_1} : \lambda_{GBS_2} : \lambda_{GBS_3} = 6 : 3 : 1$, and the two cases of periods $T = 50, N = 50$ and $T = 100, N = 100$ are compared.

As shown in the Fig. 2, as the number of users increase from 10 to 80, the minimum throughput of cell-edge users is decreasing. It can be seen from the Fig.2 that the result

Authorized licensed use limited to: Beijing Information Science & Tech Univ. Downloaded on March 19,2023 at 02:47:48 UTC from IEEE Xplore. Restrictions apply.

with $T = 100, N = 100$ is far better than the case with $T = 50, N = 50$, because the larger period allows the UAV to be closer to the cell-edge user. It can also be seen from Fig.2 that the minimum throughput decreases rapidly at beginning. This is because the distribution of 10 users may be in a relatively small range of the entire area at the beginning. As the number of users increases, the area of user distribution continues to expand. The range that UAV needs to cover is rapidly expanding, while UAV can only serve users in r_{UAV} within each slot.

As Fig. 3 show, we compare three algorithms as T increases. Furthermore, the number of users in three cells is 20 and 80, respectively. It can be seen from the Fig.3 that as the T increases, the minimum throughput increases significantly. This is because that the UAV can be closer to the user as the T increases. However, as T continues to increase, UAV will hover near some points most of the time, so the minimum throughput tends to be flat. In the case of a large number of users, the algorithm proposed in this paper is far superior to the comparison algorithm. The increase of T has no effect on the situation of only GBSs.

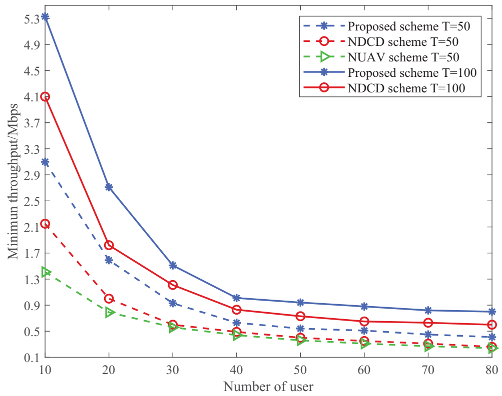

Fig. 2. Minimum throughput with different number of users.

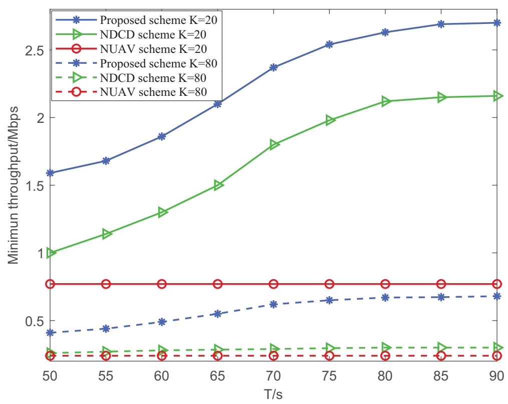

Fig. 3. Minimum throughput with different T.

TABLE I
THE NUMBER OF USERS

Case	1	2	3	4	5	6	7	8
BS1	14	12	11	10	10	9	8	7
BS2	5	6	6	8	5	9	6	7
BS3	1	2	3	2	5	2	6	6

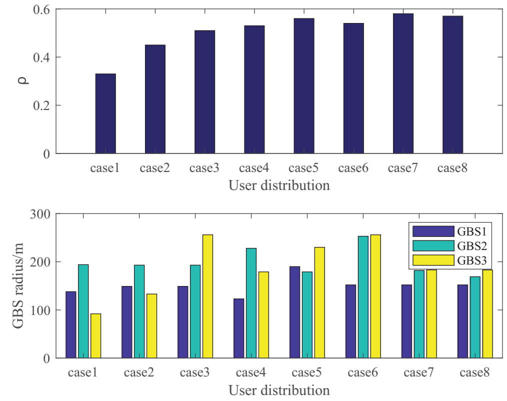

Fig. 4. Optimal results of spectrum allocation and GBSs coverage.

We assume 8 user density cases (as shown in TABLE I) to compare the parameter optimization results. As shown in Fig.4, when the number of users is large, the coverage area of the GBS is generally small. Because UAV has the opportunity to cover more users. The result as the fifth case in the Fig.4 illustrates that the number of users in cell 1 is plentiful, but the coverage of its GBS is high than cell 2 with fewer users. The coverage radius of the GBS is not proportional to the number of users covered. In order to accurately display the coverage of each GBS and UAV, as shown in Fig.6, we count the number of users covered by GBSs and UAV in each case.

To compare the UAV's trajectories in different situations, the number of users are $\lambda_{GBS_1} : \lambda_{GBS_1} : \lambda_{GBS_1} = 6 : 3 : 1$, $\lambda_{GBS_1} : \lambda_{GBS_2} : \lambda_{GBS_3} = 3 : 1 : 1$, and $\lambda_{GBS_1} : \lambda_{GBS_2} : \lambda_{GBS_3} = 7 : 7 : 6$, respectively. T is assumed to be 50s and 100s. Fig.5 illustrates that the UAV stays longer in a cell with more users. By comparing the results of the UAV trajectory under the different T, it can be found that the UAV can approach the user as close as possible when the T is large, to provide better services.

Fig.7 shows the convergence of this algrothms under the diffierent number of users. It can be seen from this figure that the convergence is almost unaffected by parameter changes.

V. CONCLUSION AND OUTLOOK

In this paper, we propose to dynamically divide the coverage between GBSs and UAV, design algorithms to optimize coverage division, spectrum allocation, and the trajectory of UAV at the edges of multiple cells. Firstly, we propose a cooperative system model between GBSs and UAV. Secondly, we derive the problem as a non-convex optimization problem and obtain

Authorized licensed use limited to: Beijing Information Science & Tech Univ. Downloaded on March 19,2023 at 02:47:48 UTC from IEEE Xplore. Restrictions apply.

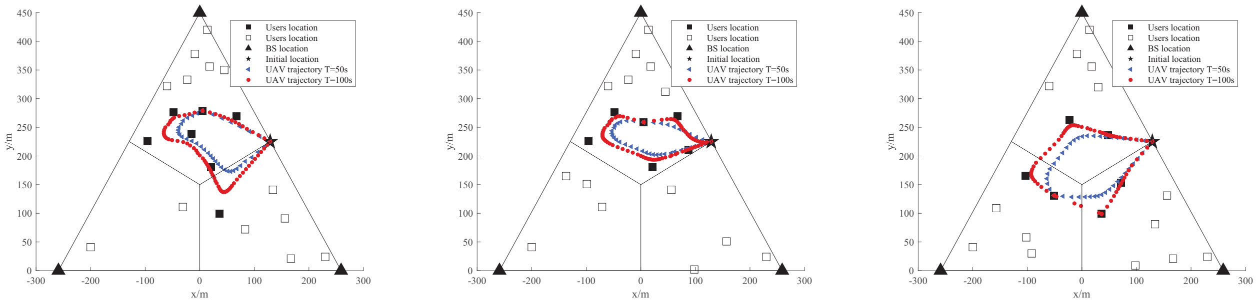

(a) Case one (b) Case two (c) Case three

Fig. 5. Trajectory of UAV.

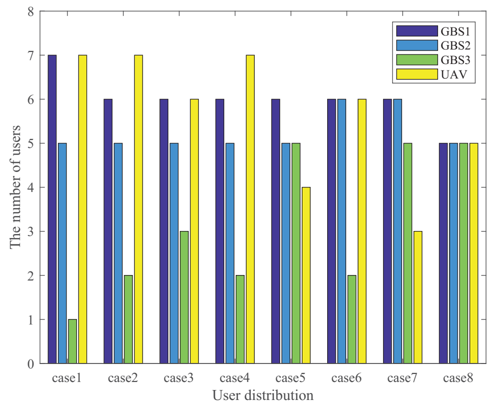

Fig. 6. The number of users served by GBSs and UAV.

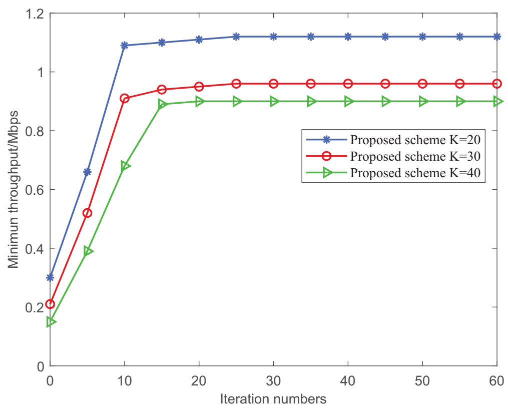

Fig. 7. Convergence analysis with different number of users.

the suboptimal solution through an iterative algorithm. Finally, by comparing with other algorithms in simulation, the strategy proposed in this paper is proved to be effective in improving the throughput of cell-edge users. In future work, we will study how to improve the energy efficiency of UAVs.

VI. Acknowledgement

This work is supported by the National Natural Science Foundation of China (Grant No.61771070).

References

[1] B. Li, Z. Fei and Y. Zhang, "UAV Communications for 5G and Beyond: Recent Advances and Future Trends," in *IEEE Internet of Things Journal*, vol. 6, no. 2, pp. 2241-2263, April 2019.

[2] J. Lyu, Y. Zeng and R. Zhang, "UAV-Aided Offloading for Cellular Hotspot," in *IEEE Transactions on Wireless Communications*, vol. 17, no. 6, pp. 3988-4001, June 2018.

[3] A. Fotouhi et al., "Survey on UAV Cellular Communications: Practical Aspects, Standardization Advancements, Regulation, and Security Challenges," in *IEEE Communications Surveys & Tutorials*, vol. 21, no. 4, pp. 3417-3442, Fourthquarter 2019.

[4] M. Mozaffari, W. Saad, M. Bennis, Y. Nam and M. Debbah, "A Tutorial on UAVs for Wireless Networks: Applications, Challenges, and Open Problems," in *IEEE Communications Surveys & Tutorials*, vol. 21, no. 3, pp. 2334-2360, thirdquarter 2019.

[5] L. Zhang et al., "A Survey on 5G Millimeter Wave Communications for UAV-Assisted Wireless Networks," in *IEEE Access*, vol. 7, pp. 117460-117504, 2019.

[6] Q. Song, F. Zheng and S. Jin, "Multiple UAVs Enabled Data Offloading for Cellular Hotspots," *2019 IEEE Wireless Communications and Networking Conference (WCNC)*, Marrakesh, Morocco, 2019, pp. 1-6.

[7] X. Li, H. Yao, J. Wang, X. Xu, C. Jiang and L. Hanzo, "A Near-Optimal UAV-Aided Radio Coverage Strategy for Dense Urban Areas," in *IEEE Transactions on Vehicular Technology*, vol. 68, no. 9, pp. 9098-9109, Sept. 2019.

[8] J. Lyu, Y. Zeng and R. Zhang, "Spectrum Sharing and Cyclical Multiple Access in UAV-Aided Cellular Offloading," *GLOBECOM 2017 - 2017 IEEE Global Communications Conference*, Singapore, 2017, pp. 1-6.

[9] J. Lyu, Y. Zeng and R. Zhang, "UAV-Aided Offloading for Cellular Hotspot," in *IEEE Transactions on Wireless Communications*, vol. 17, no. 6, pp. 3988-4001, June 2018.

[10] M. Hua, Y. Wang, C. Li, Y. Huang and L. Yang, "Energy-Efficient Optimization for UAV-Aided Cellular Offloading," in *IEEE Wireless Communications Letters*, vol. 8, no. 3, pp. 769-772, June 2019.

[11] S. Zhu, L. Gui, N. Cheng, F. Sun and Q. Zhang, "Joint Design of Access Point Selection and Path Planning for UAV-Assisted Cellular Networks," in *IEEE Internet of Things Journal*, vol. 7, no. 1, pp. 220-233, Jan. 2020.

[12] Q. Wu, Y. Zeng and R. Zhang, "Joint Trajectory and Communication Design for UAV-Enabled Multiple Access," *GLOBECOM 2017 - 2017 IEEE Global Communications Conference*, Singapore, 2017, pp. 1-6.

[13] X. Wang, H. Zhang and V. C. M. Leung, "Modeling and Performance Analysis of UAV-Assisted Cellular Networks in Isolated Regions," *2018 IEEE International Conference on Communications Workshops (ICC Workshops)*, Kansas City, MO, 2018, pp. 1-6.

[14] F. Cheng et al., "UAV Trajectory Optimization for Data Offloading at the Edge of Multiple Cells," in *IEEE Transactions on Vehicular Technology*, vol. 67, no. 7, pp. 6732-6736, July 2018.

Authorized licensed use limited to: Beijing Information Science & Tech Univ. Downloaded on March 19,2023 at 02:47:48 UTC from IEEE Xplore. Restrictions apply.